

# Comparative Electrochemical Study of Unsubstituted and Substituted Bis(phthalocyaninato) Rare Earth(III) Complexes

Peihua Zhu,<sup>[a]</sup> Fanli Lu,<sup>[a]</sup> Na Pan,<sup>[a]</sup> Dennis P. Arnold,<sup>\*,[b]</sup> Shuyong Zhang,<sup>[a]</sup> and Jianzhuang Jiang<sup>\*,[a,c]</sup>

**Keywords:** Phthalocyanines / Sandwich complexes / Rare earths / Electrochemistry

The electrochemistry of homoleptic substituted phthalocyaninato rare earth double-decker complexes  $M(\text{TBPC})_2$  and  $M(\text{OOPc})_2$  [ $M = \text{Y, La...Lu}$  except  $\text{Pm}$ ;  $\text{H}_2\text{TBPC} = 3(4), 12(13), 21(22), 30(31)$ -tetra-*tert*-butylphthalocyanine,  $\text{H}_2\text{OOPc} = 3,4,12,13,21,22,30,31$ -octakis(octyloxy)phthalocyanine] has been comparatively studied by cyclic voltammetry (CV) and differential pulse voltammetry (DPV) in  $\text{CH}_2\text{Cl}_2$  containing 0.1 M tetra-*n*-butylammonium perchlorate (TBAP). Two quasi-reversible one-electron oxidations and three or four quasi-reversible one-electron reductions have been revealed for these neutral double-deckers of two series of substituted complexes, respectively. For comparison, unsubstituted bis(phthalocyaninato) rare earth analogues  $M(\text{Pc})_2$  ( $M = \text{Y, La...Lu}$  except  $\text{Pm}$ ;  $\text{H}_2\text{Pc} = \text{phthalocyanine}$ ) have also been electrochemically investigated. Two quasi-reversible one-electron oxidations and up to five quasi-reversible one-electron reductions have been revealed for these neutral double-decker compounds. The three bis(phthalocyaninato)cerium compounds display one cerium-centered redox wave between the first ligand-based oxidation and reduction. The half-wave potentials of the first and second oxidations and first reduction for double-deckers of the tervalent rare earths depend on the size of the metal center. The difference between the redox potentials of the second and third reductions for  $M^{\text{III}}(\text{Pc})_2$ , which represents the potential difference between the first oxidation and first reduction of  $[M^{\text{III}}(\text{Pc})_2]^-$ , lies in the range 1.08–1.37 V and also gradually diminishes along with the lanthanide contraction, indicating enhanced  $\pi$ – $\pi$  interactions in the double-deckers connected by the smaller, lanthanides. This corresponds well with the red-shift of the lowest energy band observed in the electronic absorption spectra of reduced double-decker  $[M^{\text{III}}(\text{Pc}')_2]^-$  ( $\text{Pc}' = \text{Pc, TBPC, OOPc}$ ).

(© Wiley-VCH Verlag GmbH & Co. KGaA, 69451 Weinheim, Germany, 2004)

## Introduction

Bis(phthalocyaninato) rare earth compounds have been extensively studied due to their potential applications for electronic devices.<sup>[1,2]</sup> Their electrochemical properties, especially those of lutetium compounds, have been intensively investigated in solutions or in aqueous  $\text{LiClO}_4$ ,  $\text{KClO}_4$ , or  $\text{KCl}$  in cast, Langmuir–Blodgett, or spin-coated films by several research groups. These data are relevant to the use in electrochromic displays and molecular electronics of  $\text{Lu}(\text{Pc})_2$ .<sup>[1–5]</sup> As noted by Simon and co-workers,<sup>[6]</sup> the gap between the first oxidation and first reduction processes of molecules is a good estimate of the thermal activation en-

ergy for the conduction of electric charges in the solid-state materials derived from these molecular precursors.

The spectroscopic properties, namely IR,<sup>[7]</sup> Raman,<sup>[8]</sup> and electronic absorption spectra,<sup>[9]</sup> of these sandwich-type (tetrapyrrole)metal compounds depend on the strong electronic interaction between the macrocycles, which in turn depends on the ring-to-ring distances in the molecules. Therefore it is worth studying systematically the electrochemical properties of the sandwich compounds of the complete series of rare earths for various ligands. So far, we have studied the molecular structures, NMR and vibrational spectroscopic characteristics of several series of tetrapyrrole compounds with the whole series of lanthanides from La to Lu.<sup>[7–10]</sup> The groups of Konami,<sup>[11]</sup> Iwase<sup>[12]</sup> and Homborg<sup>[13]</sup> have reported the NMR, electrochemical and electronic absorption properties of reduced double-deckers of the lanthanide series, namely  $[\text{Bu}_4\text{N}][\text{M}(\text{Pc})_2]$ ,  $\text{Li}[\text{M}(\text{Pc})_2]$  and  $[\text{N}(\text{C}_n\text{H}_{2n+1})_4][\text{M}(\text{Pc})_2]$ , respectively. However, there is still no report on electrochemical investigations over the whole lanthanide series for the neutral bis(phthalocyaninato) species. The literature on any solution properties of the neutral unsubstituted bis-

<sup>[a]</sup> Department of Chemistry, Shandong University, Jinan 250100, China  
Fax: (internat.) + 86-531-856-5211  
E-mail: jzjiang@sdu.edu.cn

<sup>[b]</sup> School of Physical and Chemical Sciences, Queensland University of Technology,  
G. P. O. Box 2434, Brisbane 4001, Australia  
Fax: (internat.) + 61-7-3864-1804  
E-mail: d.arnold@qut.edu.au

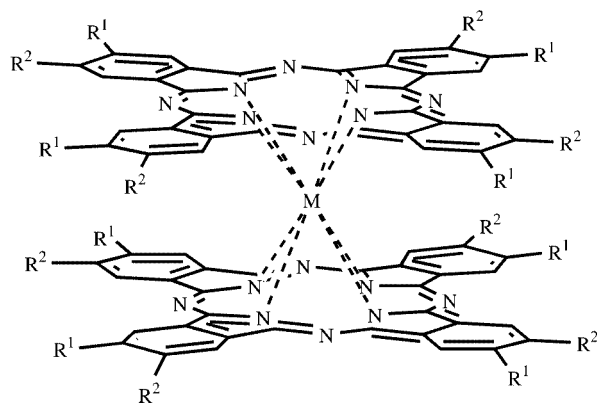
<sup>[c]</sup> State Key Lab of Coordination Chemistry, Nanjing University, Nanjing 210093, China

(phthalocyaninato) rare earth complexes is not rich due to the limited solubility of  $M(\text{Pc})_2$  in common organic solvents such as  $\text{CH}_2\text{Cl}_2$ . Investigations of the electrochemical properties of substituted bis(phthalocyaninato) rare earth compounds are also scarce, being limited to  $M(\text{OPPC})_2$  ( $M = \text{Eu}, \text{Gd}$ ),<sup>[14]</sup>  $M(\text{OHPc})_2$  ( $M = \text{Eu}, \text{Gd}$ ),<sup>[14]</sup>  $M(\text{OBPc})_2$  ( $M = \text{Yb}, \text{Lu}$ )<sup>[4d]</sup> and  $\text{Lu}(\text{TBPC})_2$ .<sup>[4c]</sup> The ligand abbreviations are given in Table 1.

Table 1. Abbreviations for ligands

Abbreviation	Ligand
$\text{H}_2\text{Por}$	general porphyrin
$\text{H}_2\text{TBPP}$	5,10,15,20-tetrakis(4- <i>tert</i> -butylphenyl)porphyrin
$\text{H}_2\text{OEP}$	2,3,7,8,12,13,17,18-octaethylporphyrin
$\text{H}_2\text{Pc}$	phthalocyanine
$\text{H}_2\text{TBPC}$	2(3),9(10),16(17),24(25)-tetra- <i>tert</i> -butylphthalocyanine
$\text{H}_2\text{OOPc}$	2,3,9,10,16,17,24,25-octakis(octyloxy)phthalocyanine
$\text{H}_2\text{OPPC}$	2,3,9,10,16,17,24,25-octakis(pentyloxy)phthalocyanine
$\text{H}_2\text{OHPc}$	2,3,9,10,16,17,24,25-octakis(heptyl)phthalocyanine
$\text{H}_2\text{OBPc}$	2,3,9,10,16,17,24,25-octakis(butyloxy)phthalocyanine
$\text{H}_2(2,3\text{-Nc})$	2,3-naphthalocyanine (linearly annulated tetrabenzophthalocyanine)
$\text{H}_2(2,3\text{-TBNc})$	3(4),12(13),21(22),30(31)-tetra- <i>tert</i> -butyl-2,3-naphthalocyanine

We report here on two series of substituted bis(phthalocyaninato)lanthanide compounds,  $M(\text{OOPc})_2$  and  $M(\text{TBPC})_2$ , whose solubility in  $\text{CH}_2\text{Cl}_2$  is significantly improved due to the introduction of extended or bulky substituents onto the Pc rings (Scheme 1). The electrochemical characterization of these substituted bis(phthalocyaninato) compounds of the whole series of lanthanides has been achieved using a glassy carbon disk working electrode. For comparison, the corresponding unsubstituted analogues  $M(\text{Pc})_2$  have also been prepared and investigated electrochemically. These unsubstituted counterparts also show recognizable and reproducible electrochemical features under the present conditions although the cyclic and differential pulse voltammograms are not resolved as clearly as those of the substituted analogues  $M(\text{TBPC})_2$  and  $M(\text{OOPc})_2$ . By comparison between the electrochemical characteristics of unsubstituted and substituted bis(phthalocyaninato) com-



Scheme 1. Bis(phthalocyaninato) rare earth complexes  $\text{R}^1 = \text{R}^2 = \text{H}$ ,  $M(\text{Pc})_2$  (A);  $\text{R}^1 \neq \text{R}^2 = \text{H}$ , *tert*- $\text{C}_4\text{H}_9$ ,  $M(\text{TBPC})_2$  (B);  $\text{R}^1 = \text{R}^2 = \text{OC}_8\text{H}_{17}$ ,  $M(\text{OOPc})_2$  (C)

pounds of the whole series of lanthanides, the effects of ionic radius of the rare earth metal and substituents (*tert*-butyl and octyloxy groups) on the electrochemical properties of double-decker compounds have been studied.

More redox couples can be revealed by using the glassy carbon disk due to the decreased interaction or affinity between the highly charged electrochemically generated complexes and the electrode.<sup>[12b,15]</sup> The same methodology has been applied here to render possible the first observation by DPV of the fifth one-electron reduction of  $M(\text{Pc})_2$  in solution.<sup>[15]</sup>

## Results and Discussion

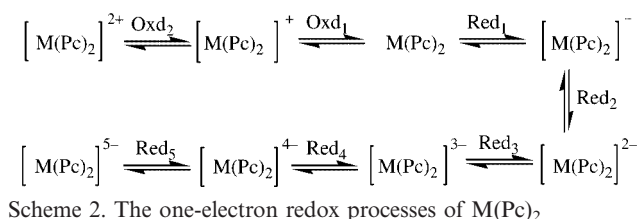
### Electrochemical Characteristics of Bis(phthalocyaninato) Rare Earth Complexes $M(\text{Pc})_2$ ( $M = \text{Y}, \text{La} \dots \text{Lu}$ except Pm)

The electrochemical behavior of all the double-decker sandwich complexes  $M(\text{Pc})_2$  was first investigated by cyclic voltammetry (CV) and then differential pulse voltammetry (DPV) in  $\text{CH}_2\text{Cl}_2$ . The half-wave redox potentials vs. SCE are summarized in Table 2. Figure 1 shows the cyclic voltammograms and differential pulse voltammograms of  $\text{Y}(\text{Pc})_2$  as a typical representative of this series of rare earth compounds. The cyclic voltammograms of other compounds in the same series are similar. Within the electrochemical window of  $\text{CH}_2\text{Cl}_2$  and according to the CV and DPV results, all the double-decker compounds of trivalent rare earths except Lu undergo two quasi-reversible one-electron oxidations and up to five quasi-reversible one-electron reductions under the present conditions. The separation of the reduction and oxidation peak potentials for each process is 60–95 mV. Since the oxidation state of the central trivalent rare earth ion does not change (except for  $M = \text{Ce}$ ), these processes are due to successive removal or addition of electrons from or to the ligand-based orbitals that are represented by the redox states illustrated in Scheme 2, where oxidations are labeled as  $\text{Oxd}_1$  and  $\text{Oxd}_2$  and the reductions as  $\text{Red}_1$  to  $\text{Red}_5$ .

The electrochemistry of the unsubstituted double-deckers in  $\text{CH}_2\text{Cl}_2$  seen here differs from that previously reported. For instance, only three or at most four reductions were observed for  $\text{Lu}(\text{Pc})_2$  in  $\text{CH}_2\text{Cl}_2$  or benzonitrile (PhCN) containing  $\text{TBAPF}_6$ .<sup>[4]</sup> However, under our experimental conditions, the neutral bis(phthalocyaninato) compounds of trivalent rare earths undergo up to five one-electron reductions according to both the CV and, more clearly, the DPV results.

The effect of rare earth ion size is clearly demonstrated by the slight shift in the negative direction of the half-wave potentials of the first oxidation and first reduction of  $M^{\text{III}}(\text{Pc})_2$  with decreasing rare earth ion radius. Moreover, a linear correlation exists between the potentials of the first oxidation and first reduction and the trivalent rare earth ionic radii (Figure 2). The half-wave potentials of the second oxidation also depend on the ionic radius of the central rare earth metal (Figure 2). However, the slope of this

	Oxd <sub>2</sub>	Oxd <sub>1</sub>	Red <sub>1</sub>	Red <sub>2</sub>	Red <sub>3</sub>	Red <sub>4</sub>	Red <sub>5</sub>	$\Delta E^\circ_{1/2}$ <sup>[a]</sup>	$\Delta E^{\circ'}_{1/2}$ <sup>[b]</sup>
La	+1.34	+0.61	+0.27	−1.10	−1.31	−1.55 <sup>[c]</sup>	−1.85 <sup>[c]</sup>	0.34	1.37
Ce	+1.04 <sup>[d]</sup>	+0.55 <sup>[d]</sup>	+0.09 <sup>[e]</sup>	−1.10 <sup>[f]</sup>	−1.31 <sup>[c]</sup> <sup>[f]</sup>			0.49 <sup>[g]</sup>	1.19
Pr	+1.34	+0.58	+0.22	−1.15	−1.39	−1.68 <sup>[c]</sup>	−1.80 <sup>[c]</sup>	0.36	1.37
Nd	+1.49 <sup>[c]</sup>	+0.56	+0.15	−1.12	−1.34	−1.63 <sup>[c]</sup>	−1.74 <sup>[c]</sup>	0.41	1.27
Sm	+1.56	+0.56	+0.14	−1.11	−1.33	−1.60 <sup>[c]</sup>	−1.74 <sup>[c]</sup>	0.42	1.25
Eu	+1.59	+0.55	+0.12	−1.07	−1.29	−1.54 <sup>[c]</sup>	−1.70 <sup>[c]</sup>	0.43	1.19
Gd	+1.57 <sup>[c]</sup>	+0.52	+0.11	−1.08	−1.30	−1.53 <sup>[c]</sup>	−1.72 <sup>[c]</sup>	0.41	1.19
Tb	+1.60 <sup>[c]</sup>	+0.51	+0.09	−1.08	−1.32	−1.53	−1.66 <sup>[c]</sup>	0.42	1.17
Dy	+1.50	+0.47	+0.07	−1.09	−1.30	−1.57 <sup>[c]</sup>	−1.83 <sup>[c]</sup>	0.40	1.16
Y	+1.61	+0.47	+0.06	−1.11	−1.35	−1.66 <sup>[c]</sup>	−1.81 <sup>[c]</sup>	0.41	1.17
Ho		+0.47	+0.04	−1.10	−1.36	−1.70 <sup>[c]</sup>	−1.88 <sup>[c]</sup>	0.43	1.14
Er	+1.63	+0.47	+0.06	−1.09	−1.35	−1.60 <sup>[c]</sup>	−1.75 <sup>[c]</sup>	0.41	1.15
Tm	+1.54	+0.45	+0.05	−1.07	−1.29	−1.54 <sup>[c]</sup>	−1.75 <sup>[c]</sup>	0.40	1.12
Yb	+1.64 <sup>[c]</sup>	+0.44	+0.02	−1.09	−1.32			0.42	1.11
Lu	+1.60 <sup>[c]</sup>	+0.40	−0.02	−1.10 <sup>[c]</sup>	−1.33 <sup>[c]</sup>	−1.58 <sup>[c]</sup>		0.42	1.08



Detailed description of Figure 1: The graph plots the standard reduction potential  $E_{1/2}$  in Volts (V) on the y-axis against the ionic radius  $r_{ion}$  in picometers (pm) on the x-axis. The x-axis ranges from 98 to 116 pm with major ticks every 2 units. The y-axis ranges from -2.00 to 2.00 V with major ticks every 0.50 units. There are seven data series:   
 1. **Oxd2**: Represented by filled squares. It starts at approximately 1.60 V at 98 pm and decreases to about 1.30 V at 116 pm.   
 2. **Oxd1**: Represented by filled circles. It starts at approximately 0.40 V at 98 pm and increases to about 0.60 V at 116 pm.   
 3. **Red1**: Represented by open circles. It starts at approximately 0.00 V at 98 pm and increases to about 0.30 V at 116 pm.   
 4. **Red2**: Represented by filled triangles. It remains relatively constant around -1.30 V.   
 5. **Red3**: Represented by open triangles. It remains relatively constant around -1.30 V.   
 6. **Red4**: Represented by filled diamonds. It remains relatively constant around -1.10 V.   
 7. **Red5**: Represented by open diamonds. It remains relatively constant around -1.80 V.   
 Some data points for Red2, Red3, Red4, and Red5 are missing at certain radii, indicated by gaps in the series.

Ionic radii (pm)	Oxd2 (V)	Oxd1 (V)	Red1 (V)	Red2 (V)	Red3 (V)	Red4 (V)	Red5 (V)
98	1.60	0.40	0.00	-1.30	-1.30	-1.10	-1.80
99	1.65	0.40	0.05	-1.30	-1.30	-1.10	-1.80
100	1.60	0.40	0.05	-1.30	-1.30	-1.10	-1.80
101	1.55	0.40	0.05	-1.30	-1.30	-1.10	-1.80
102	1.60	0.40	0.05	-1.30	-1.30	-1.10	-1.80
103	1.50	0.40	0.05	-1.30	-1.30	-1.10	-1.80
104	1.60	0.45	0.05	-1.30	-1.30	-1.10	-1.80
105	1.55	0.45	0.10	-1.30	-1.30	-1.10	-1.80
106	1.55	0.45	0.10	-1.30	-1.30	-1.10	-1.80
107	1.55	0.45	0.10	-1.30	-1.30	-1.10	-1.80
108	1.55	0.45	0.10	-1.30	-1.30	-1.10	-1.80
109	1.50	0.40	0.15	-1.30	-1.30	-1.10	-1.80
110	1.45	0.40	0.20	-1.30	-1.30	-1.10	-1.80
111	1.45	0.40	0.20	-1.30	-1.30	-1.10	-1.80
112	1.30	0.40	0.25	-1.30	-1.30	-1.10	-1.80
113	1.30	0.40	0.25	-1.30	-1.30	-1.10	-1.80
114	1.25	0.40	0.30	-1.30	-1.30	-1.10	-1.80
115	1.25	0.40	0.30	-1.30	-1.30	-1.10	-1.80
116	1.30	0.60	0.30	-1.30	-1.30	-1.10	-1.80

The potential difference between the first oxidation and first reduction process,  $\Delta E^{\circ}_{1/2}$ , for all double-decker compounds  $M(\text{Pc})_2$  spans a relatively narrow range, 0.34–0.43 V, which accords well with previously reported results for bis(phthalocyaninato)lutetium compounds.<sup>[4]</sup> This potential

difference is important for molecular materials because it predicts electrical properties such as the thermal activation energy for conduction in the condensed phases derived from these molecular precursors.<sup>[6]</sup> As with  $\text{Lu}(\text{Pc})_2$ , the unsubstituted bis(phthalocyaninato) rare earth compounds should be good molecular semi-conductors based on the small potential difference between their first oxidation and first reduction.

X-ray crystallographic studies of bis(phthalocyaninato) rare earth compounds show that the two isoindole  $\text{N}_4$  planes are very close to each other (2.68–3.11 Å).<sup>[1a]</sup> This proximity of the two conjugated  $\pi$ -systems in a face-to-face configuration causes the monomer molecular orbitals to split, which can be demonstrated by studying the redox behavior and the optical properties (UV/Vis, near-IR and MCD spectra). Figure 3 shows a qualitative scheme for the frontier orbitals of  $\text{M}(\text{Pc})_2$  derived from the highest occupied and lowest unoccupied molecular orbitals (HOMO and LUMO) of  $\text{M}(\text{Pc})_2$ .<sup>[16,17]</sup> The LUMO of mono(metallophthalocyanines) is doubly degenerate ( $e_g$ ) and can accept up to four electrons; this is also true for the LUMO of the bis(phthalocyaninato) rare earth compounds. The HOMO of the homoleptic phthalocyaninato double-deckers results from a splitting of the  $4a_u$   $\pi$ -HOMO of the mono(phthalocyanines) due to the interactions between the rings. Thus, in the neutral complexes consisting of a tervalent metal ion sandwiched between (formally) a dianion and an anion radical, the HOMO is semi-occupied. These neutral bis(phthalocyaninato) compounds of tervalent rare earths are thus expected to be reducible by a total of five electrons as confirmed by the above-described electrochemical measurements. This orbital proposal is well supported by the optical properties, especially in the near-IR range of  $\text{M}(\text{Pc})_2$ .<sup>[18]</sup> The bis(phthalocyaninato) tervalent rare earth complexes

are known to be neutral radicals, the HOMO being semi-occupied. The absorption band at ca. 920 nm in the electronic spectrum, which shows an  $A$ -Faraday-type band in the MCD spectrum, is attributed to the electronic transition from the semi-occupied HOMO to the degenerate LUMO. The absorption to even lower energy at ca. 1400 nm is due to the transition from the second HOMO to the semi-occupied HOMO.<sup>[18]</sup> This energy represents the extent of electronic coupling between the macrocycles, since the electron correlation energy term vanishes due to the semi-occupation of the HOMO. This absorption band becomes increasingly blue-shifted with the lanthanide contraction, indicating that decreasing rare earth ionic size induces increasing ring-to-ring interaction and more profound splitting between the HOMO and second HOMO of double-deckers (Figure 3), and thus there is an increase in the energy of the HOMO and a decrease in that of the second HOMO. This is why the half-wave potentials of the second oxidation ( $\text{Oxd}_2$ ) are shifted slightly in a more positive direction with decreasing rare earth ion radius, whereas those for the first oxidation and first reduction of  $\text{M}^{\text{III}}(\text{Pc})_2$ ,  $\text{Oxd}_1$  and  $\text{Red}_1$ , are shifted slightly in the negative direction in the same order.

According to the orbital scheme depicted in Figure 3,  $\Delta E^{\circ}_{1/2}$  (0.34–0.43 V) represents the energy for putting a second electron in the semi-occupied HOMO of the neutral double-decker radical  $\text{M}(\text{Pc})_2$  or to remove one electron of the two from the HOMO of the reduced double-decker species  $[\text{M}(\text{Pc})_2]^-$ . In other words, it is the energy for pairing the two electrons in the HOMO of  $[\text{M}(\text{Pc})_2]^-$ , and it remains almost unchanged for the whole series of lanthanides. The corresponding energy for removing one electron of the two from the HOMO of  $\text{Ce}(\text{Pc})_2$ , 0.49 V, is slightly higher compared to that for  $[\text{M}(\text{Pc})_2]^-$  because of the smaller ionic size of the intermediate valence state of cerium and, thus, the more intense ring–ring interaction in  $\text{Ce}(\text{Pc})_2$ . This is also true for substituted bis(phthalocyaninato)cerium complexes (Tables 3 and 4).

Furthermore, the difference of the redox potentials of  $\text{Red}_2$  and  $\text{Red}_3$  for  $\text{M}(\text{Pc})_2$  actually corresponds to the potential difference between the first oxidation and first reduction of  $[\text{M}(\text{Pc})_2]^-$ ,  $\Delta E^{\circ'}_{1/2}$ . The values range from 1.08 to 1.37 V across the series, and gradually diminish along with decreasing rare earth ion radius, clearly showing a size effect and indicating the enhanced  $\pi$ – $\pi$  interactions in the double-deckers with smaller lanthanides compared with those connected by larger lanthanides (Table 2). The same general trend is also found for the substituted bis(phthalocyaninato) rare earth analogues  $\text{M}(\text{TBPC})_2$  and  $\text{M}(\text{OOPc})_2$  (see Table 4). As the first oxidation step and first reduction step, respectively, involve the HOMO and the LUMO of the molecule, the energy difference between these two redox processes for  $[\text{M}(\text{Pc})_2]^-$  corresponds to its electrochemical molecular band gap. Thus  $\Delta E^{\circ'}_{1/2}$  should reflect the energy necessary for the transition of an electron from the HOMO to the LUMO of  $[\text{M}(\text{Pc})_2]^-$  and therefore should correlate with the lowest energy optical transition in the electronic absorption spectrum of  $[\text{M}(\text{Pc})_2]^-$ . In fact, the diminished

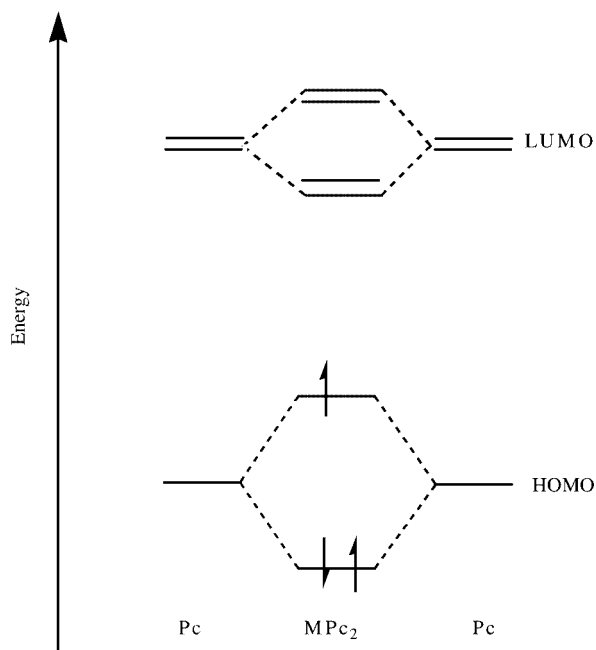


Figure 3. Frontier orbitals of  $\text{M}(\text{Pc})_2$



Table 3. Half-wave redox potentials of M(TBPC)<sub>2</sub> (V vs. SCE) in CH<sub>2</sub>Cl<sub>2</sub> containing 0.1 M TBAP

	Oxd <sub>2</sub>	Oxd <sub>1</sub>	Red <sub>1</sub>	Red <sub>2</sub>	Red <sub>3</sub>	Red <sub>4</sub>	$\Delta E^{\circ}_{1/2}$ <sup>[a]</sup>	$\Delta E^{\circ'}_{1/2}$ <sup>[b]</sup>
La	+1.36	0.52	0.14	−1.18	−1.43		0.38	1.32
Ce	+0.91 <sup>[c]</sup>	+0.42 <sup>[c]</sup>	−0.03 <sup>[d]</sup>	−1.16 <sup>[e]</sup>	−1.41 <sup>[e]</sup>	−1.84 <sup>[e]</sup> <sup>[f]</sup>	0.49 <sup>[g]</sup>	1.13
Pr	+1.39	+0.49	+0.10	−1.14	−1.37	−1.76 <sup>[f]</sup>	0.39	1.24
Nd	+1.46	+0.48	+0.08	−1.15 <sup>[f]</sup>	−1.36 <sup>[f]</sup>	−1.79 <sup>[f]</sup>	0.40	1.23
Sm	+1.48	+0.46	+0.05	−1.13	−1.36 <sup>[f]</sup>	−1.72 <sup>[f]</sup>	0.41	1.18
Eu	+1.50	+0.45	+0.03	−1.13	−1.36	−1.74	0.42	1.16
Gd	+1.48	+0.42	+0.01	−1.15	−1.40 <sup>[f]</sup>	−2.00 <sup>[f]</sup>	0.41	1.16
Tb	+1.51	+0.41	−0.03	−1.20	−1.49 <sup>[f]</sup>	−1.88 <sup>[f]</sup>	0.44	1.17
Dy	+1.51	+0.39	−0.04	−1.15	−1.40 <sup>[f]</sup>		0.43	1.11
Y	+1.57	+0.40	+0.01	−1.14	−1.44	−1.80 <sup>[f]</sup>	0.41	1.14
Ho	+1.57	+0.37	−0.07	−1.20	−1.47 <sup>[f]</sup>	−1.89 <sup>[f]</sup>	0.44	1.13
Er	+1.56	+0.37	−0.05	−1.13	−1.38	−1.92 <sup>[f]</sup>	0.42	1.08
Tm	+1.53 <sup>[c]</sup>	+0.35	−0.08	−1.14	−1.40	−1.90 <sup>[f]</sup>	0.43	1.06
Yb	+1.55	+0.35	−0.11	−1.19	−1.50 <sup>[f]</sup>	−1.94 <sup>[f]</sup>	0.46	1.08
Lu	+1.56	+0.35	−0.10	−1.19	−1.48	−1.80	0.45	1.09

<sup>[a]</sup>  $\Delta E^{\circ}_{1/2}$  is the energy needed to put a second electron in the semi-occupied HOMO of the neutral double-decker radical M(TBPC)<sub>2</sub> or to remove one electron of the two from the HOMO of the reduced double-decker species [M(TBPC)<sub>2</sub>]<sup>−</sup>:  $\Delta E^{\circ}_{1/2} = \text{Oxd}_1 - \text{Red}_1$ . <sup>[b]</sup>  $\Delta E^{\circ'}_{1/2}$  is the potential difference between the first oxidation and first reduction processes, i.e. the HOMO–LUMO gap of [M(TBPC)<sub>2</sub>]<sup>−</sup>:  $\Delta E^{\circ'}_{1/2} = \text{Red}_1 - \text{Red}_2$ . <sup>[c]</sup> This process involves an intermediate cerium CeX species, where x is between iii and iv. <sup>[d]</sup> Involves a cerium-centered redox process. <sup>[e]</sup> Involves a Ce<sup>III</sup> species. <sup>[f]</sup> Recorded by DPV. <sup>[g]</sup> For Ce(TBPC)<sub>2</sub>:  $\Delta E^{\circ}_{1/2} = \text{Oxd}_2 - \text{Oxd}_1$ .

Table 4. Half-wave redox potentials of M(OOPC)<sub>2</sub> (V vs. SCE) in CH<sub>2</sub>Cl<sub>2</sub> containing 0.1 M TBAP

	Oxd <sub>2</sub>	Oxd <sub>1</sub>	Red <sub>1</sub>	Red <sub>2</sub>	Red <sub>3</sub>	$\Delta E^{\circ}_{1/2}$ <sup>[a]</sup>	$\Delta E^{\circ'}_{1/2}$ <sup>[b]</sup>
La	+1.20	+0.46	+0.10	−1.31	−1.63	0.36	1.41
Ce	+0.78 <sup>[c]</sup>	+0.33 <sup>[c]</sup>	−0.18 <sup>[d]</sup>			0.45 <sup>[e]</sup>	
Pr	+1.23	+0.42	+0.01	−1.31	−1.64 <sup>[f]</sup>	0.41	1.33
Nd	+1.25	+0.40	0.00	−1.28	−1.60 <sup>[f]</sup>	0.40	1.28
Sm	+1.26	+0.40	−0.01	−1.29	−1.65 <sup>[f]</sup>	0.41	1.28
Eu	+1.33	+0.36	−0.06	−1.29	−1.71	0.42	1.23
Gd	+1.40	+0.35	−0.07	−1.27	−1.56 <sup>[f]</sup>	0.42	1.20
Tb	+1.38	+0.33	−0.10	−1.30	−1.60 <sup>[f]</sup>	0.43	1.20
Dy	+1.35	+0.32	−0.11	−1.30	−1.66	0.43	1.19
Y	+1.40	+0.31	−0.12	−1.31	−1.69	0.43	1.19
Ho	+1.47	+0.31	−0.11	−1.29	−1.65 <sup>[f]</sup>	0.42	1.18
Er		+0.30	−0.13	−1.30	−1.59 <sup>[f]</sup>	0.43	1.17
Tm	+1.51 <sup>[f]</sup>	+0.29	−0.15	−1.31 <sup>[c]</sup>	−1.67 <sup>[f]</sup>	0.44	1.16
Yb	+1.51 <sup>[f]</sup>	+0.28	−0.15	−1.26	−1.62	0.43	1.12
Lu	+1.47	+0.27	−0.17	−1.30	−1.71	0.44	1.13

<sup>[a]</sup>  $\Delta E^{\circ}_{1/2}$  is the energy needed to put a second electron in the semi-occupied HOMO of the neutral double-decker radical M(OOPC)<sub>2</sub> or to remove one electron of the two from the HOMO of the reduced double-decker species [M(OOPC)<sub>2</sub>]<sup>−</sup>:  $\Delta E^{\circ}_{1/2} = \text{Oxd}_1 - \text{Red}_1$ . <sup>[b]</sup>  $\Delta E^{\circ'}_{1/2}$  is the potential difference between the first oxidation and first reduction processes, i.e. the HOMO–LUMO gap of [M(OOPC)<sub>2</sub>]<sup>−</sup>:  $\Delta E^{\circ'}_{1/2} = \text{Red}_1 - \text{Red}_2$ . <sup>[c]</sup> This process involves an intermediate cerium CeX species, where x is between iii and iv. <sup>[d]</sup> Involves a cerium-centered redox process. <sup>[e]</sup> For Ce(OOPC)<sub>2</sub>:  $\Delta E^{\circ}_{1/2} = \text{Oxd}_2 - \text{Oxd}_1$ . <sup>[f]</sup> Recorded by DPV.

trend observed for  $\Delta E^{\circ'}_{1/2}$  of bis(phthalocyaninato)metal complexes along with the rare earth contraction is in good agreement with the red-shift of the lowest electronic absorption band of [M(Pc)<sub>2</sub>]<sup>−</sup>, 682 nm for M = Sm to 705 nm for M = Lu, along with the same order.

The cerium double-decker is particularly interesting because of its anomalous electrochemical and spectroscopic properties. As indicated by electronic absorption, Raman

and <sup>1</sup>H NMR studies, both phthalocyanine rings seem to exist as dianions in bis(phthalocyaninato)cerium, Ce(Pc<sup>2−</sup>)<sub>2</sub>, while the valence state of the cerium ion appears to be intermediate between iii and iv from XNAFS data. This anomaly is due to the strong hybridization of the 4f orbital of cerium with the  $\pi$  orbitals of conjugated phthalocyanine ligands.<sup>[19]</sup> The CV and DPV studies of Ce(Pc<sup>2−</sup>)<sub>2</sub> show five distinct redox waves that represent quasi-reversible single-electron processes. The second and third reduction peaks at −1.10 and −1.31 V, respectively, are related to the successive addition of electrons to the ligand-based orbitals that are represented by the redox states [Ce(Pc)<sub>2</sub>]<sup>−</sup>/[Ce(Pc)<sub>2</sub>]<sup>2−</sup> and [Ce(Pc)<sub>2</sub>]<sup>2−</sup>/[Ce(Pc)<sub>2</sub>]<sup>3−</sup>, in which the cerium ion seems to be tervalent, because both potentials correspond with those of the rest of the series M<sup>III</sup>(Pc)<sub>2</sub> [M ≠ Ce] (Table 2 and Figure 2). The anomalous reduction wave at +0.09 V thus appears to be metal-centered: [Ce<sup>III</sup>(Pc<sup>2−</sup>)<sub>2</sub>]<sup>−</sup>/[Ce<sup>x</sup>(Pc<sup>n−</sup>)<sub>2</sub>], where x is between iii and iv, and n is an average formal charge such as to maintain the required net charge.<sup>[19]</sup> The anomalous (with respect to the other lanthanides) electronic structure of cerium and the strong hybridization of the 4f orbitals with the ligand orbitals make the metal-centered redox process (here either the addition, or the removal, of one electron to, or from, a 4f orbital of the cerium ion) dependent on the nature of the phthalocyanine rings. Therefore, the half-wave potential of the cerium-based redox process for Ce(Pc)<sub>2</sub> differs from that for Ce(TBPC)<sub>2</sub> and Ce(OOPC)<sub>2</sub> [Tables 3 and 4 (see below)], following the logical order 0.09, −0.03, −0.18 as the ligands become more electron-donating and thus the metal centre becomes harder to reduce. The first and second oxidation processes at +0.55 and +1.04 V for Ce(Pc)<sub>2</sub> involve successive removal of electrons from the ligand-based HOMO that are represented by the redox states: [Ce<sup>x</sup>(Pc)<sub>2</sub>]/[Ce<sup>x</sup>(Pc)<sub>2</sub>]<sup>+</sup> and [Ce<sup>x</sup>(Pc)<sub>2</sub>]<sup>+</sup>/[Ce<sup>x</sup>(Pc)<sub>2</sub>]<sup>2+</sup>

(in which again a fractional average formal charge must be assigned to the ligands to maintain the overall charge). The cerium ion in these redox states has the same formal charge as in  $[\text{Ce}(\text{Pc})_2]^0$  because both potentials deviate significantly from the linear relationship established between the potentials of corresponding redox processes, actually the first reduction and first oxidation of  $\text{M}^{\text{III}}(\text{Pc})_2$ , and the rare earth ion radii (Table 2 and Figure 2).

**Electrochemical Characteristics of Bis[3(4),12(13),21(22),30(31)-tetra-*tert*-butylphthalocyaninato] Rare Earth Complexes  $\text{M}(\text{TBPC})_2$  ( $\text{M} = \text{Y}, \text{La} \dots \text{Lu}$  except Pm)**

The bis[3(4),12(13),21(22),30(31)-tetra-*tert*-butylphthalocyaninato] rare earth complexes  $\text{M}(\text{TBPC})_2$ , which are substituted by four *tert*-butyl groups on the periphery of each phthalocyanine macrocycle, are actually a mixture of isomers, all of which seem to have the same electrochemical properties. This has been confirmed by the electrochemical behavior of other bis(phthalocyaninato)lutetium or bis(naphthalocyaninato) rare earth compounds, tetrasubstituted on the periphery of each (na)phthalocyanine ring.<sup>[4c,9c]</sup>

Similar to the unsubstituted analogues, CV and DPV have revealed two ligand-centered quasi-reversible one-electron oxidations and up to four ligand-centered quasi-reversible one-electron reductions for  $\text{M}^{\text{III}}(\text{TBPC})_2$ . The incorporation of the four electron-donating *tert*-butyl groups onto each phthalocyanine ring makes the compounds easier to oxidize and harder to reduce. This is well demonstrated by the lower oxidation and reduction half-wave potentials of the corresponding redox processes of  $\text{M}(\text{TBPC})_2$  compared with those of  $\text{M}(\text{Pc})_2$  (Table 3 and Figure 4). The cathodic shift of all the processes means that only four reductions were observed for  $\text{M}(\text{TBPC})_2$ . The fifth reduction process observed for  $\text{M}(\text{Pc})_2$  under the same experimental conditions could not be seen. This is also the case for  $\text{M}(\text{OOPc})_2$  as discussed below. Moreover, since these *tert*-butyl-substituted bis(phthalocyaninato) rare earth complexes are more soluble in alkyl halides such as  $\text{CH}_2\text{Cl}_2$  compared with  $\text{M}(\text{Pc})_2$ , the measurement of their properties in solution is more favorable. This is verified by the improved resolution of the redox couples in most of the voltammograms. Figure 4 displays the CV and DPV diagrams of  $\text{Ce}(\text{TBPC})_2$ , in which the sensitivity is seen to be better than for  $\text{M}(\text{Pc})_2$ .

The dependence of the half-wave potentials of the redox processes on the ionic size of the central rare earth ion is similar for  $\text{M}(\text{TBPC})_2$  to that for  $\text{M}(\text{Pc})_2$  (Table 3). While the half-wave potentials of the second, third and fourth reductions of  $\text{M}(\text{TBPC})_2$  are independent of the size of the central rare earth ions, the potentials for the second and first oxidations and first reduction are size-sensitive, but the opposite slope is observed for the first process compared with the other two.

The small electron-pairing energy for  $\text{M}(\text{TBPC})_2$ ,  $\Delta E_{1/2}^\circ$  (0.38–0.46 V), which corresponds well with those of corresponding  $\text{M}(\text{Pc})_2$  and  $\text{M}(\text{OOPc})_2$  (see below), indicates that

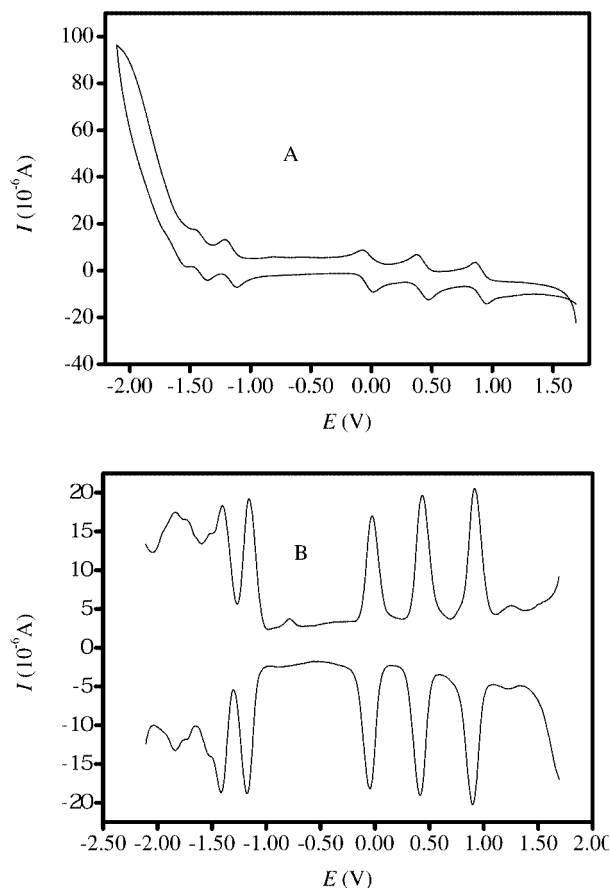


Figure 4. CV (A) and DPV (B) of  $\text{Ce}(\text{TBPC})_2$  in  $\text{CH}_2\text{Cl}_2$  containing 0.1 M  $[\text{Bu}_4\text{N}][\text{ClO}_4]$  at scan rates 20 and 10  $\text{mV s}^{-1}$ , respectively

these substituted bis(phthalocyaninato) rare earth compounds should be good potential molecular semi-conductors, as expected for their unsubstituted analogues. Due to their increased solubility in common organic solvents, by virtue of the *tert*-butyl groups, these compounds would be more easily fabricated into electronic devices by solution fabrication methods. The similar  $\Delta E_{1/2}^\circ$  values for  $\text{M}(\text{TBPC})_2$  to those of the unsubstituted counterparts indicates that the pairing energy in the HOMO of  $[\text{M}(\text{TBPC})_2]^-$  is quite similar to that for the HOMO of  $[\text{M}(\text{Pc})_2]^-$  although the redox potentials of the first oxidation and first reduction processes of  $\text{M}(\text{TBPC})_2$  shift cathodically due to the introduction of electron-donating *tert*-butyl groups. This is also true for  $\text{M}(\text{OOPc})_2$ .

Furthermore, according to the decreasing  $\Delta E_{1/2}^\circ$  value of  $\text{M}(\text{TBPC})_2$  with decreasing rare earth ionic radius (Table 3), a red-shift in the lowest energy band of reduced tetra-*tert*-butyl-substituted bis(phthalocyaninato) rare earth compounds  $[\text{M}(\text{TBPC})_2]^-$  ( $\text{M} = \text{Sm} \dots \text{Lu}$ ) should be expected to follow in the same order. In fact, the lowest energy band for  $[\text{M}(\text{TBPC})_2]^-$  shifts from 688 nm for  $\text{M} = \text{Sm}$  to 714 nm for  $\text{M} = \text{Lu}$ . This is also true for  $[\text{M}(\text{OOPc})_2]^-$ .<sup>[9d]</sup>

As clearly shown in the CV and DPV spectra of  $\text{Ce}(\text{TBPC})_2$  (Figure 4) and on the basis of comparison between the electrochemical data of  $\text{Ce}(\text{TBPC})_2$  and those of

$M^{III}(TBPC)_2$  (Table 3), the same Ce redox states apply here as for  $Ce(Pc)_2$  [and also for  $Ce(OOPc)_2$  (Table 4)].

### Electrochemical Characteristics of Bis[3,4,12,13,21,22,30,31-octakis(octyloxy)phthalocyaninato] Rare Earth Complexes $M(OOPc)_2$ ( $M = Y, La...Lu$ Except Pm)

Very similar electrochemical behavior to that of  $M(Pc)_2$  and  $M(TBPC)_2$  has been revealed by CV and DPV methods for bis[3,4,12,13,21,22,30,31-octakis(octyloxy)phthalocyaninato] rare earth complexes  $M(OOPc)_2$  (Table 4). The introduction of eight octyloxy groups, which are more electron-donating than the four *tert*-butyl groups, means that the double-deckers  $M(OOPc)_2$  become easier to oxidize and harder to reduce, therefore showing lower first and second oxidation potentials and more negative first, second and third reduction potentials than the corresponding analogues  $M(TBPC)_2$ . Due to the additional shift of corresponding redox processes of  $M(OOPc)_2$  to a more negative direction than those of  $M(TBPC)_2$ , only three reduction processes were observed within the electrochemical window of  $CH_2Cl_2$  for the former. Under similar experimental conditions, only one one-electron oxidation and two one-electron reductions were observed by Takahashi<sup>[4d]</sup> for the butyloxy-substituted bis(phthalocyaninato) rare earth analogues  $M(OBPc)_2$  ( $M = Yb, Lu$ ).

As can be seen from Table 4, discussion for  $Ce(OOPc)_2$  is prevented due to the failure to record the half-wave potential for the second reduction process by either CV or DPV.

## Conclusions

The five quasi-reversible one-electron reductions observed within the electrochemical window of  $CH_2Cl_2$  for the unsubstituted bis(phthalocyaninato) rare earth complexes  $M^{III}(Pc)_2$  ( $M \neq Ce, Pm, Yb, Lu$ ) demonstrate again that the LUMO of bis(phthalocyaninato) rare earth compounds is doubly degenerate and can accept up to four electrons, while the HOMO of the bis(phthalocyaninato) trivalent rare earth complexes is semi-occupied and can accept one electron. However, only three and four quasi-reversible one-electron reductions were observed for  $M^{III}(OOPc)_2$  and  $M^{III}(TBPC)_2$ , respectively, under the same experimental conditions, due to the shift of corresponding redox potentials in a negative direction induced by the introduction of electron-donating octyloxy or *tert*-butyl groups. As usual, the Ce complexes are exceptional due to the unique oxidation state of the central metal ion. One cerium-centered redox wave could easily be distinguished from the CV and DPV diagrams of these three bis(phthalocyaninato)cerium compounds. Systematic studies of the electrochemical characteristics of unsubstituted, tetra-*tert*-butyl- and octakis(octyloxy)-substituted bis(phthalocyaninato) complexes of the whole trivalent lanthanide series clearly indicate that the half-wave potentials, in particular the first oxidation and first reduction processes, are all metal-ion-size-depen-

dent. The change in the half-wave potentials of these redox processes is apparently due to stronger inter-ligand interactions and generally tighter bonding as the metal ion radius contracts across the series. In the next paper in this series the corresponding data for heteroleptic tris(phthalocyaninato) rare earth(III) triple-deckers are reported and analyzed.<sup>[20]</sup>

## Experimental Section

Homoleptic bis(phthalocyaninato) rare earth double-decker compounds  $M(Pc)_2$ ,  $M(OOPc)_2$  and  $M(TBPC)_2$  were prepared according to published procedures.<sup>[9d,14,21]</sup> CV and DPV measurements were carried out with a BAS CV-50 W voltammetric analyzer. The cell consists of inlets for a glassy carbon disk working electrode (2.0 mm diameter) and a silver-wire counter electrode. The reference electrode was  $Ag/Ag^+$  connected to the solution by a Luggin capillary whose tip was placed close to the working electrode. Results are corrected for junction potentials by being referenced internally to the ferrocenium/ferrocene ( $Fe^+/Fe$ ) couple [ $E_{1/2}(Fe^+/Fe) = +0.50$  V vs. SCE]. The potentials in this paper are referenced to the SCE. Typically, a 0.1 M solution of  $[Bu_4N][ClO_4]$  in  $CH_2Cl_2$  containing 0.5 mM sample was purged with nitrogen for 10 min; the voltammograms were then recorded at ambient temperature with scan rates of 20 and 10 mV/s for CV and DPV, respectively.

## Acknowledgments

The authors thank the National Natural Science Foundation of China (Grant No. 20171028), the National Ministry of Science and Technology of China (Grant No. 2001CB6105-04), The Science Committee of Shandong Province (Grant No. Z99B03), the National Educational Ministry of China, Shandong University, and Queensland University of Technology for financial support.

- [1a] J. Jiang, K. Kasuga, D. P. Arnold, in *Supramolecular Photosensitive and Electroactive Materials* (Ed.: H. S. Nalwa), Academic Press, New York, **2001**, chapter 2, pp. 113–210. [1b] D. K. P. Ng, J. Jiang, *Chem. Soc. Rev.* **1997**, 26, 433–442. [1c] J. Jiang, W. Liu, D. P. Arnold, *J. Porphyrins Phthalocyanines* **2003**, 7, 459–473.
- [2] J. W. Buchler, D. K. P. Ng, in *The Porphyrin Handbook* (Eds.: K. M. Kadish, K. M. Smith, R. Guilard), Academic Press, New York, **1999**, chapter 20, pp. 245–294.
- [3] [3a] M. M. Nicholson, in *The Phthalocyanines: Properties and Applications* (Eds.: C. C. Leznoff, A. B. P. Lever), VCH Publishers, New York, **1993**, vol. 3, pp. 76–117. [3b] P. M. S. Monk, R. J. Mortimer, D. R. Rosseinsky, in *Electrochromism: Fundamentals and Applications* (Eds.: P. Gregory, U. Anton), VCH Publishers, Weinheim, **1995**.
- [4] [4a] M. L'Her, Y. Cozien, J. Courtot-Coupez, *J. Electroanal. Chem.* **1983**, 157, 183–187. [4b] F. Castaneda, C. Piechocki, V. Plichon, J. Simon, J. Vaxiviere, *Electrochim. Acta* **1986**, 31, 131–133. [4c] A. Pondaven, Y. Cozien, M. L'Her, *New J. Chem.* **1991**, 15, 515–516. [4d] K. Takahashi, Y. Tomita, Y. Hada, K. Tsubota, M. Handa, K. Kasuga, K. Sogabe, T. Tokii, *Chem. Lett.* **1992**, 759–762. [4e] F. Guyon, A. Pondaven, P. Guenot, M. L'Her, *Inorg. Chem.* **1994**, 33, 4787. [4f] M. L'Her, Y. Cozien, J. Courtot-Coupez, *C. R. Acad. Sci. Ser. 2* **1986**, 302, 9–14.
- [5] [5a] G. C. S. Collins, D. J. Schiffrin, *J. Electroanal. Chem.* **1982**, 139, 335–369. [5b] S. Besbes, V. Pichon, J. Simon, J. Vaxiviere,

- J. Electroanal. Chem.* **1987**, 237, 61–68. <sup>[5c]</sup> F. Castaneda, V. Plichon, *J. Electroanal. Chem.* **1987**, 236, 163–175. <sup>[5d]</sup> M. Bardin, E. Bertounesque, V. Plichon, J. Simon, V. Ahsen, O. Bekaroglu, *J. Electroanal. Chem.* **1989**, 271, 173–180. <sup>[5e]</sup> Y. Liu, K. Shigehara, M. Hara, A. Yamada, *J. Am. Chem. Soc.* **1991**, 113, 440–443. <sup>[5f]</sup> T. Toupance, V. Plichon, J. Simon, *New J. Chem.* **1999**, 23, 1001–1006.
- [6] <sup>[6a]</sup> J. Simon, J. J. Andre, *Molecular Semi-conductors*, Springer Verlag, Berlin, Germany, **1985**. <sup>[6b]</sup> M. Bouvet, J. Simon, *Chem. Phys. Lett.* **1990**, 172, 299–302.
- [7] <sup>[7a]</sup> J. Jiang, D. P. Arnold, H. and Yu, *Polyhedron* **1999**, 8, 2129–2139. <sup>[7b]</sup> X. Sun, M. Bao, N. Pan, X. Cui, D. P. Arnold, J. Jiang, *Aust. J. Chem.* **2002**, 9, 587–595. <sup>[7c]</sup> F. Lu, M. Bao, C. Ma, X. Zhang, D. P. Arnold, J. Jiang, *Spectrochim. Acta Part A*, in press.
- [8] <sup>[8a]</sup> J. Jiang, L. Rintoul, D. P. Arnold, *Polyhedron* **2000**, 19, 1381–1394. <sup>[8b]</sup> J. Jiang, U. Cornelissen, D. P. Arnold, X. Sun, H. Homborg, *Polyhedron* **2001**, 20, 557–569. <sup>[8c]</sup> N. Pan, L. Rintoul, D. P. Arnold, J. Jiang, *Polyhedron* **2002**, 21, 1905–1912. <sup>[8d]</sup> Y. Bian, L. Rintoul, D. P. Arnold, N. Pan, J. Jiang, *Vib. Spectrosc.* **2003**, 31, 173–185. <sup>[8e]</sup> X. Sun, L. Rintoul, Y. Bian, D. P. Arnold, R. Wang, J. Jiang, *J. Raman Spectrosc.* **2003**, 34, 306–314.
- [9] <sup>[9a]</sup> J. Jiang, Y. Bian, F. Furuya, W. Liu, M. T. M. Choi, H. W. Li, N. Kobayashi, Q. Yang, T. C. W. Mak, D. K. P. Ng, *Chem. Eur. J.* **2001**, 7, 5059–5069. **2003**, 27, 844–849. <sup>[9b]</sup> J. Jiang, W. Liu, K. L. Cheng, K. W. Poon, D. K. P. Ng, *Eur. J. Inorg. Chem.* **2001**, 413–417. <sup>[9c]</sup> J. Jiang, W. Liu, K. W. Poon, D. Du, D. P. Arnold, D. K. P. Ng, *Eur. J. Inorg. Chem.* **2000**, 205–209. <sup>[9d]</sup> W. Liu, J. Jiang, D. Du, D. P. Arnold, *Aust. J. Chem.* **2000**, 53, 131–136.
- [10] Y. Bian, D. Wang, R. Wang, L. Wen, J. Dou, D. Zhao, D. K. P. Ng, J. Jiang, *New J. Chem.* **2003**, 27, 844–849.
- [11] <sup>[11a]</sup> H. Konami, H. Hatano, N. Kobayashi, T. Osa, *Chem. Phys. Lett.* **1990**, 165, 397–400. <sup>[11b]</sup> H. Konami, H. Hatano, A. Tajiri, *Chem. Phys. Lett.* **1989**, 160, 163–167.
- [12] <sup>[12a]</sup> A. Iwase, C. Harnood, Y. Kameda, *J. Alloys Compds.* **1993**, 192, 280–283. <sup>[12b]</sup> C. Harnood, F. Kitamura, T. Ohsaka, K. Tokuda, A. Iwase, *Denki Kagaku* **1993**, 61, 767–769.
- [13] <sup>[13a]</sup> M. S. Haghighi, H. Homborg, *Z. Anorg. Allg. Chem.* **1994**, 620, 1278–1284. <sup>[13b]</sup> G. Ostendorp, H. Homborg, *Z. Anorg. Allg. Chem.* **1996**, 622, 1222–1230.
- [14] J. Jiang, R. C. W. Liu, T. C. W. Mak, T. W. D. Chan, D. K. P. Ng, *Polyhedron* **1997**, 16, 515–520.
- [15] K. M. Kadish, T. Nakanishi, A. Gürek, V. Ahsen, I. Yilmaz, *J. Phys. Chem. B* **2001**, 105, 9817–9821.
- [16] <sup>[16a]</sup> E. Orti, J. L. Bredas, *J. Chem. Phys.* **1990**, 92, 1228–1235. <sup>[16b]</sup> R. Rousseau, R. Aroca, M. L. Rodriguez-Mendez, *J. Mol. Struct.* **1995**, 356, 49–62. <sup>[16c]</sup> N. Ishikawa, *J. Porphyrins Phthalocyanines* **2001**, 5, 87–101.
- [17] <sup>[17a]</sup> A. Giraudeau, A. Louati, M. Gross, J. J. Andre, J. Simon, H. C. Su, K. M. Kadish, *J. Am. Chem. Soc.* **1983**, 105, 2917–2919. <sup>[17b]</sup> A. Louati, M. El Meray, J. J. Andre, J. Simon, K. M. Kadish, M. Gross, A. Giraudeau, *Inorg. Chem.* **1995**, 24, 1175–1179.
- [18] N. Kobayashi, personal communication.
- [19] <sup>[19a]</sup> W. Kuchle, M. Dolg, H. Stoll, *J. Phys. Chem.* **1997**, 101, 7128–7133. <sup>[19b]</sup> Y. Bian, J. Jiang, Y. Tao, M. T. M. Choi, R. Li, A. C. H. Ng, P. Zhu, N. Pan, X. Sun, D. P. Arnold, Z. Zhou, H.-W. Li, D. K. P. Ng, *J. Am. Chem. Soc.* **2003**, 125, 12257–12267. <sup>[19c]</sup> H. Homborg, personal communications.
- [20] P. Zhu, N. Pan, C. Ma, X. Sun, D. P. Arnold, J. Jiang, *Eur. J. Inorg. Chem.*, accepted.
- [21] J. Jiang, J. Xie, M. T. M. Choi, D. K. P. Ng, *J. Porphyrins Phthalocyanines* **1999**, 3, 322–328.

Received July 28, 2003

Early View Article

Published Online December 12, 2003